DOI: 10.13009/EUCASS2017-34

Benchmark and Application of Operational Modal Analysis Techniques on Ariane 5 Flight Records

*S. Muller *, N. Marczak**, B. Troclet*** and G. Coppotelli*****

**Expert in Structural Analysis Airbus Safran Launchers, Les Mureaux, France*
stephane.muller@airbusafran-launchers.com

***Airbus Safran Launchers, Les Mureaux, France*
nicolas.marczak@airbusafran-launchers.com

****Senior Expert in Structural Analysis - Airbus Safran Launchers, Les Mureaux, France*

Professor – Ecole normale supérieure Paris-Saclay, France
bernard.troclet@airbusafran-launchers.com

*****Department of Mechanical and Aerospace Engineering - University La Sapienza, Rome - Italy*
giuliano.coppotelli@uniroma1.it

Abstract

Operational Modal Analysis (OMA) is a largely applied process in the analysis of in-situ static structures like bridges and buildings, but remains still scarcely used on launchers. A collaboration activity was engaged between Airbus Safran Launchers and La Sapienza University to implement and select the most appropriate OMA methods to take benefit of recorded data of more than 70 Ariane 5 flights. The paper details the benchmark done on different OMA techniques, their application on academic test cases and on Ariane 5 in-flight measurements. First results, conditions of use and first results led on flight measurements are presented.

1. Introduction

Technique of Operational Modal Analysis (OMA) encompasses a large spectrum of data treatments used to retrieve dynamics characteristics of structures in operations. The main targeted parameters are frequencies, mode shapes and damping whose records allow following evolution of structures in their time-life and building useful database for future development. Quantification of uncertainties in modal characteristics w.r.t. variety of solicitations, damping values attached to types of hardware, architecture and junctions are among others valuable output that can be expected from the use of OMA. Such techniques are largely used in the analysis of in-situ static structures like bridges and buildings, but also in motion vehicles like trains [5] but remains still scarcely used on launchers.

Main reasons are:

- The various excitation types that are encountered during the flights of launch vehicles, that includes long duration white noise excitation (thrust noise of engines, buffeting excitation, aerodynamic noise), transient bursts, short and combined excitations like lift-off blast wave, shocks events a.s.o. (figure 1).

- The non-stationary state of launchers in operation, whose dynamic behaviour strongly evolves during the flight (mass of launchers typically decrease by tons per second). Main dynamics recorded by vibration transducers vary during launchers flight phase. Figure 2 (from [7] and [8]) shows the evolution of the main solid rocket booster modes on Vega and Ariane 5 whose frequencies can triple during burn time.

- Limited telemetry transmission bandwidth that constraints amount of channels and precision of measurements, making number and quality of records much more limited than during ground records.

DOI: 10.13009/EUCASS2017-34

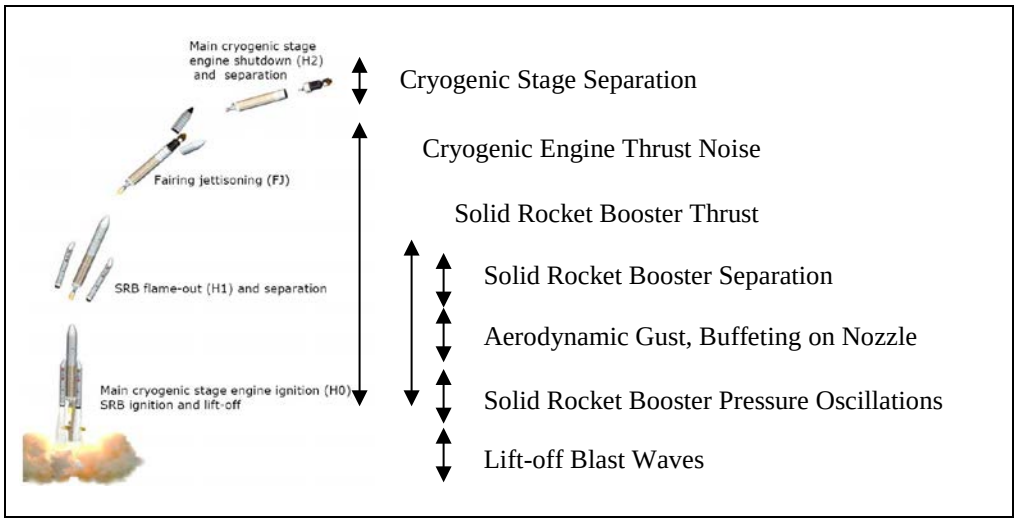

Figure 1: Excitation Encountered in Ariane 5 Flight

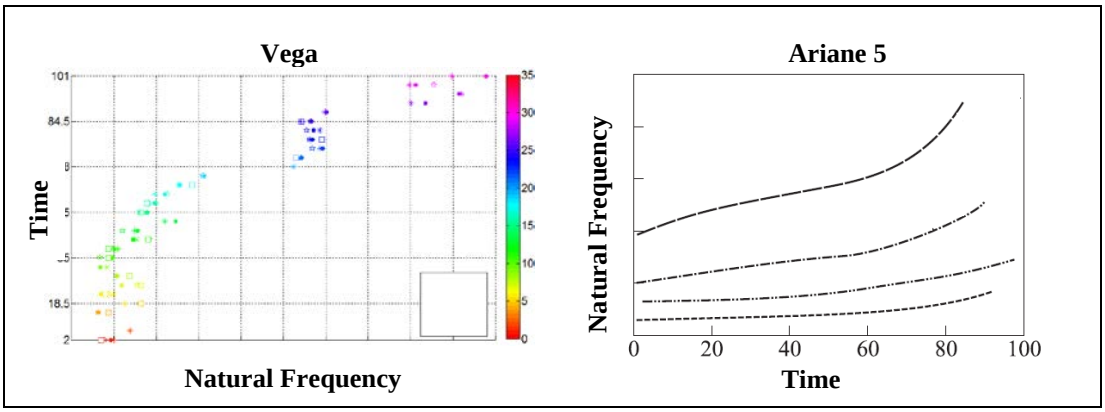

Figure 2: Main Structural Dynamics of Ariane 5 and Vega

Use of OMA on launch vehicle flight is thus very challenging. The benefit of OMA is nevertheless important as representative tests performed on hardware are limited and rarely fully representative of the operational conditions of use. OMA can give the opportunities to retrieve modal information during manufacturing, transportation phases or hot firing tests. Additionally, it can be used to capitalize on lessons-learnt of operational flights with a special focus on damping values whose accurate prediction is still an issue. Past attempts to use these techniques proved to be encouraging [1], [2] and first results were obtained from launcher measurements [3], [6].

Several OMA techniques, working in frequency and in time domain, have been developed in recent years. For launcher application, we focused on Frequency Domain Decomposition (FDD), Hilbert Transform Method (HTM) as well as two Stochastic Subspace Identification (SSI) methods: the Balanced Realization (BR) in the time domain and the SSI-f in frequency domain. The choice of these techniques was the results of a collaboration activity engaged between Airbus Safran Launchers and La Sapienza University whose details can be found in [4].

2. Theoretical Background

The dynamic motion of the analysed structure can be expressed by:

$$M\ddot{x}(t) + C\dot{x}(t) + Kx(t) = f(t) \quad \textbf{(1)}$$

M, C, K being the mass, damping and stiffness matrices, $x(t), f(t)$ the displacements and the forces time-varying vectors.

DOI: 10.13009/EUCASS2017-34

Reformulated in state-space form with $x_1(t) = \begin{Bmatrix} x(t) \\ \dot{x}(t) \end{Bmatrix}$ and $y(t) = x(t)$ then in the frequency space ω, it comes:

$$\begin{cases} \mathrm{j}\omega \mathrm{X}_1(\omega) = \mathrm{A}\mathrm{X}_1(\omega) + \mathrm{B}\mathrm{F}(\omega) \\ \mathrm{Y}(\omega) = \mathrm{D}\mathrm{X}_1(\omega) \end{cases} \quad \textbf{(2)}$$

where $A = \begin{bmatrix} 0 & I \\ -M^{-1}K & M^{-1}C \end{bmatrix}$, $B = \begin{Bmatrix} 0 \\ M^{-1} \end{Bmatrix}$ and $D = \begin{bmatrix} I & 0 \end{bmatrix}$

The Frequency Response Function (FRF) H(ω) gives the relationship between the input and output of a linear system as follows $Y(\omega) = H(\omega)F(\omega) = D\left[j\omega I - A\right]^{-1} BF(\omega)$. Introducing the right hand side eigenvector V and eigenvalue Λ of A ($AV = \Lambda V$), it comes $H(\omega) = DV\left[j\omega I - \Lambda\right]^{-1} V^{-1}B$ and finally $H(\omega) = \Psi\left[j\omega I - \Lambda\right]^{-1}\Phi^T$ where the matrices Ψ and Φ represent the mode shapes and the modal participations of the system, respectively.

If the system is weakly damped and the modes well separated in the frequency spectrum (low frequency domain), the eigenvectors are those of the undamped system and the FRF can be expressed in terms of the modal parameters :

$$\mathrm{H}(\omega) = \sum \frac{\psi^{(\mathrm{n})} \varphi^{(\mathrm{n})\mathrm{T}}}{\mathrm{j}\omega - \lambda_{\mathrm{n}}} + \frac{\psi^{(\mathrm{n})} \varphi^{(\mathrm{n})\mathrm{H}}}{\mathrm{j}\omega - \lambda_n^*} \quad \textbf{(3)}$$

λ_n, $\varphi^{(n)}$ and $\Psi^{(n)}$ being the n-th pole, mode shape and modal participation.

The output spectral density function matrix $G_{yy}(\omega)$ can then be computed from the spectral density functions and is linked to the FRF and the input spectral density $G_{xx}(\omega)$.

$$\mathrm{G}_{\mathrm{yy}}(\omega) = \begin{bmatrix} \mathrm{G}_{\mathrm{y_1y_1}}(\omega) & \ldots & \mathrm{G}_{\mathrm{y_1y_n}}(\omega) \\ . & . & . \\ \mathrm{G}_{\mathrm{y_ny_1}}(\omega) & \ldots & \mathrm{G}_{\mathrm{y_ny_n}}(\omega) \end{bmatrix} = \mathrm{H}(\omega)\ \mathrm{G}_{\mathrm{xx}}(\omega)\ \mathrm{H}^{\mathrm{H}}(\omega) \quad \textbf{(4)}$$

If we assume that the excitation is a white noise, $G_{xx}(\omega)$ becomes diagonal and the output power spectral density can be only expressed through modes shapes and modal contribution [9].

$$\mathrm{G}_{\mathrm{yy}} = \sum \frac{\psi^{(n)} \overline{\varphi}^{(\mathrm{n})\mathrm{T}}}{\mathrm{j}\omega - \lambda_{\mathrm{n}}} + \frac{\psi^{(n)} \overline{\varphi}^{(\mathrm{n})\mathrm{H}}}{\mathrm{j}\omega - \lambda_n^*} + \frac{\overline{\varphi}^{(n)} \psi^{(\mathrm{n})\mathrm{T}}}{-\mathrm{j}\omega - \lambda_{\mathrm{n}}} + \frac{\overline{\varphi}^{(n)*} \psi^{(\mathrm{n})\mathrm{H}}}{-\mathrm{j}\omega - \lambda_n^*} \quad \textbf{(5)}$$

2.1 Frequency Domain Decomposition (FDD)

The FDD uses the power spectrum density matrix $G_{yy}(\omega)$ and decompose it by the Singular Value Decomposition. If the modes are well separated, which is the case in the low frequency domain, the major contribution near a resonance point can be assimilated to one mode, the structure behaving as a single degree of freedom. Performing an inverse Fourier transformation of equation (5) in the neighbourhood of the identified natural frequency allows retrieving frequency and damping ratio by the logarithmic decrement technique.
In order to define the frequencies interval where the system behaves like a single degree of freedom, the mode shape associated to the identified frequency is compared by using the Modal Assurance Criterion (MAC) with those

DOI: 10.13009/EUCASS2017-34

associated with the neighbouring frequencies. Thus, by fixing a threshold MAC, the searched interval is obtained and the damping ratio can be identified.

2.2 Hilbert Transform Method (HTM)

The HTM use the property of the Hilbert transform applied to causal signals to estimate the FRF, its poles and then frequencies and damping of modes. Considering an uncorrelated random excitation source the FRF can be reformulated from equation (3) into $|H_{ii}(\omega)|^2 = \frac{G_{y_i y_i}(\omega)}{G_{x_i x_i}(\omega)}$.

Introducing natural logarithm and Hilbert transform $\mathcal{H}$, it comes $2\mathcal{H}[\ln|H_{ii}(\omega)|] = \mathcal{H}\left[\ln G_{y_i y_i}(\omega)\right]$ as Hilbert transform of a constant is zero. $H_{ii}(\omega)$ can be represented by a polar representation $H_{ii}(\omega) = |H_{ii}(\omega)|e^{-j\varphi_{ii}(\omega)}$. Applying natural logarithm gives $\ln(H_{ii}(\omega)) = \ln(|H_{ii}(\omega)|) - j\varphi_{ii}(\omega)$ and Hilbert properties on causal signals lead finally to: $\varphi_{ii}(\omega) = -\frac{1}{2}\mathcal{H}\left[\ln(G_{y_i y_i}(\omega))\right]$.

From the above expressions, it's possible to access to $H_{y_i y_i}(\omega)$ values. $H_{y_i y_j}(\omega)$ can then be computed [10]

$$H_{ij}(\omega) = \frac{G_{y_i y_j}(\omega)}{\sqrt{G_{x_i x_i}(\omega)}\, H^*_{ij}(\omega)} \tag{6}$$

In the frequency range of definition of the FRF, the number of modes is not known; therefore a stabilization diagram is introduced to estimate it by means of an iterative procedure.

2.3 Stochastic Subspace Identification (SSI-f) and Balanced Realization (BR) methods

The goal of the Stochastic Subspace Identification methods is the assessment of the system modal parameters through eigenvalues and the eigenvectors of the state matrix A. By definition, the observability matrix, $O_p \in \Re^{pN_0 x 2N}$ of order p, is given by:

$$O_p = \begin{bmatrix} C \\ CA \\ . \\ CA^{p-1} \end{bmatrix} \tag{7}$$

Thus, the C matrix can be pulled out by the first N_0 lines of O_p and CA from the next ones; as a result the estimation of A matrix is obtained by a least square procedure [11]. Time domain method (BR) evaluates the observability matrix by the Hankel r_1 x r_2 matrices built the following way:

$$H_{r_1 r_2} = \begin{bmatrix} R_1 & R_2 & R_3 & . & R_{r_2} \\ R_2 & R_3 & R_4 & . & . \\ R_3 & R_4 & R_5 & . & . \\ . & . & . & . & . \\ R_{r_1} & . & . & . & R_{r_1+r_2} \end{bmatrix} \tag{8}$$

Correlation factors R_i are defined by $R_i = E[y_i(k)y_i(k-1)^t]$, $y_i(k)$ being a vibration response sampled at $t_k = k\Delta t$. Frequency method (SSI-f) evaluates the observability matrix by the Vandermonde matrix using the z-transform and a given matrix factor p.

DOI: 10.13009/EUCASS2017-34

$$\begin{bmatrix} \underline{Y_-} \\ Y_+ \end{bmatrix} = \begin{bmatrix} z_1^{-p}Y_1 & z_2^{-p}Y_2 & . & z_N^{-p}Y_N \\ z_1^{-p+1}Y_1 & z_2^{-p+1}Y_2 & . & z_N^{-p+1}Y_N \\ . & . & . & \\ \underline{z_1^{-1}Y_1} & \underline{z_2^{-1}Y_2} & \underline{....} & \underline{z_N^{-1}Y_N} \\ Y_1 & Y_2 & . & Y_N \\ z_1Y_1 & z_1Y_2 & . & z_1Y_N \\ . & . & . & \\ z_1^{p-1}Y_1 & z_2^{p-1}Y_2 & . & z_2^{p-1}Y_N \end{bmatrix} \quad \textbf{(9)}$$

It is possible to demonstrate [11] that $\frac{Y_+}{Y_-} = O_p$ X. and observability can be derived.

3. Robustness of OMA Algorithms on Synthetic Test Signal

The four previously described methods were applied on a synthetic signal in order to analyse the sensitivity of results:

- to the tunings that can be applied on methods,
- to the alterations that can be encountered on recorded signals.

The impact of all these tunings and alterations has to be quantified to strengthen the reliability of results given by the different methods. The chosen signal (figure 3) is a second order response with a constant frequency of 10 Hz and damping varying from 1 to 2%.

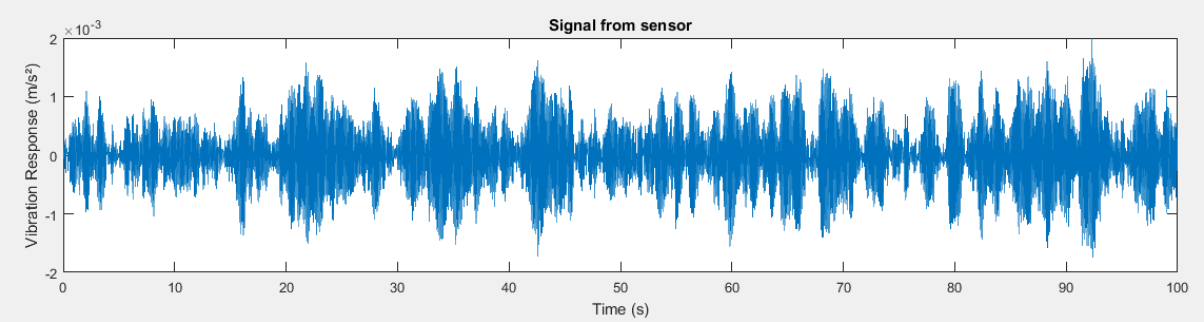

Figure 3: Synthetic Test Signal

3.1 Time Slot Duration (Applied to the Four Algorithms)

Dynamics recorded on a launcher vary strongly in flight limiting duration on which signals can be considered stationary (and thus reliably analysed). Figure 4 shows the accuracy achieved for the four methods considering different analysis durations. Whereas frequency precision is still acceptable for all methods, damping precision can be coarse on small time duration analyses. The SSI-f (and FDD in a lesser extent) appears to be less scattered; conversely HTM and BR are not well adapted as they require long duration analysis to converge through accurate values of damping.

DOI: 10.13009/EUCASS2017-34

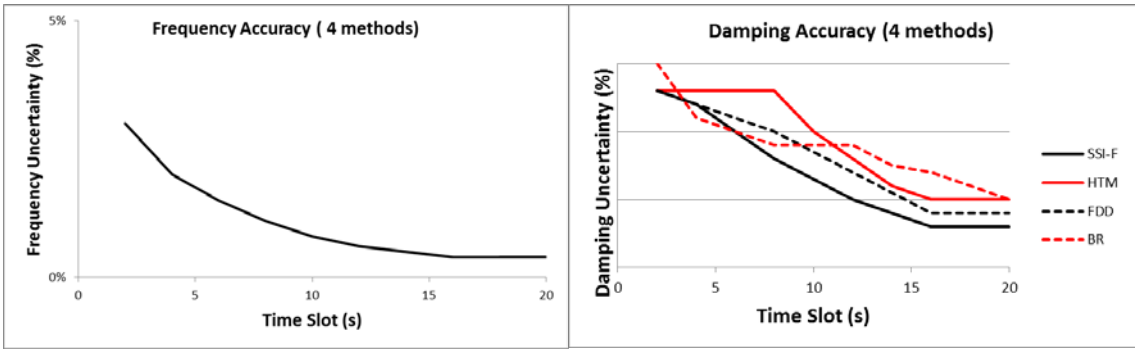

Figure 4: Accuracy vs. Time Slot Duration

3.2 Quantification of the signals (Applied to the Four Algorithms)

Quantification (e.g. Less Significant Bit LSB) of the signals is another issue specific to launcher linked to the limited available transmission bandwidth. Quantification is not as thin as what is available on ground measurements. (Figure 5, left part) from [12] illustrates the quantification of an Ariane5 flight measurement. The consequence is limited on frequency assessment but more significant on damping assessment as it increases the duration time analysis required for reliable damping assessments (Figure 5, right part).

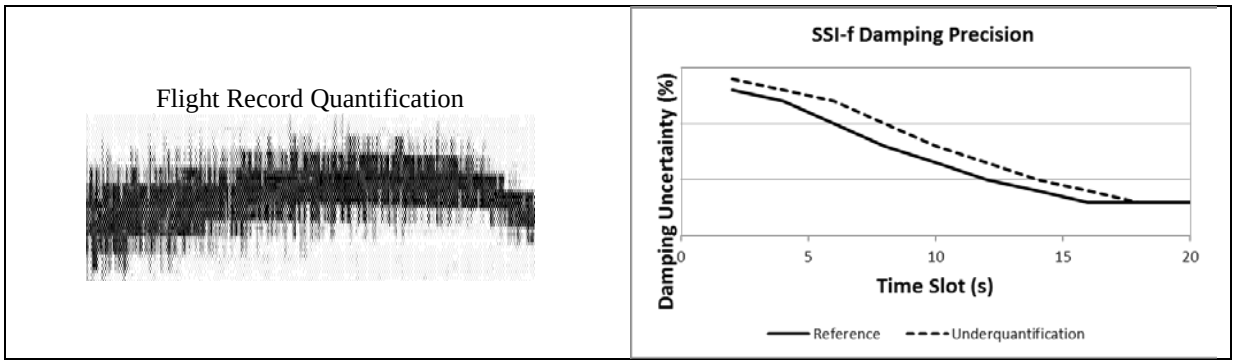

Figure 5: Accuracy vs. Quantification of the Signals

3.3 Choice of the Hankel Matrix Rank (Applied to BR Method)

The impact of the rank of the Hankel matrix (equation 8) can be quantified using ratio N/r_1 and r_1/r_2, N, r_1 and r_2 being respectively the number of samples, lines and columns. The size of the Hankel matrix is not impacting the frequency estimation. Conversely damping estimation is very sensitive to the order, important ratio N/r_1 being the most favourable case which means in practice large duration of analysis (figure.6).

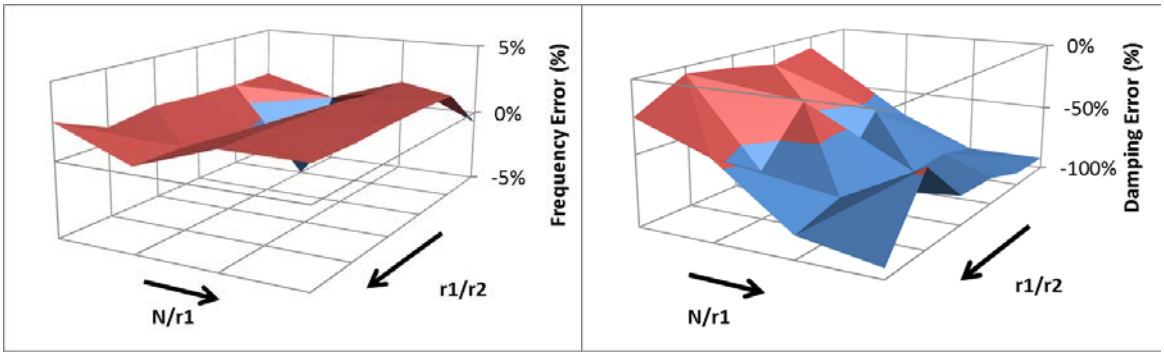

Figure 6: Accuracy vs. Hankel Matrix Rank

DOI: 10.13009/EUCASS2017-34

3.4 Choice of the Vandermonde Matrix Factor (Applied to SSI-f Method)

Using different factor p on equation 9 put in evidence that this factor is quite influent in the estimation of poles (frequency and damping diagrams on figure 7). The targeted values are highlighted by blue boxes. Small values increase the level of noise generating fictitious modes. Conversely, large values generate scattered stabilization diagrams hard to handle with.

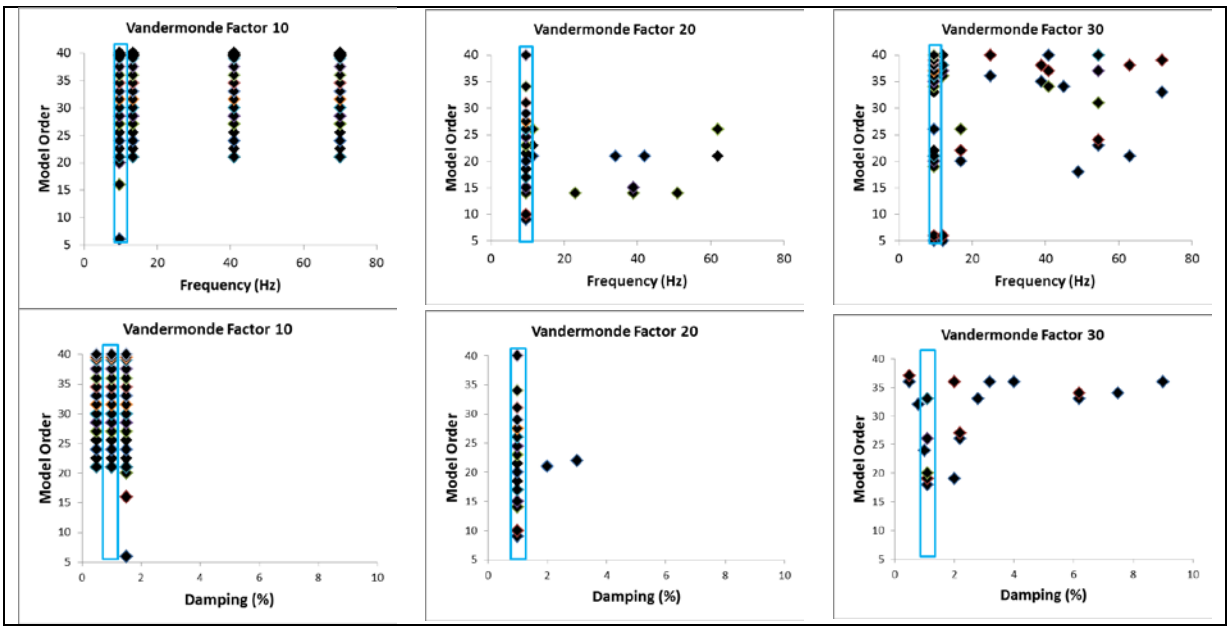

Figure 7: Accuracy vs. Vandermonde Matrix Rank

As no clear rule pop up from these tests, we recommend proceeding to several analyses with different factors to gain confidence in the analysis of the methods results.

3.5 Choice of the System Order (Applied to BR, HTM and SSI-f Methods)

The maximal order of the system drives the number of poles extracted from the signal. Figure 8 presents an illustration using SSI-f methods. A balance must be done between a too low number that doesn't allow retrieving any dynamics and a too high number that generates significant fictitious modes (red boxes) that can mask the real modes (blue boxes).

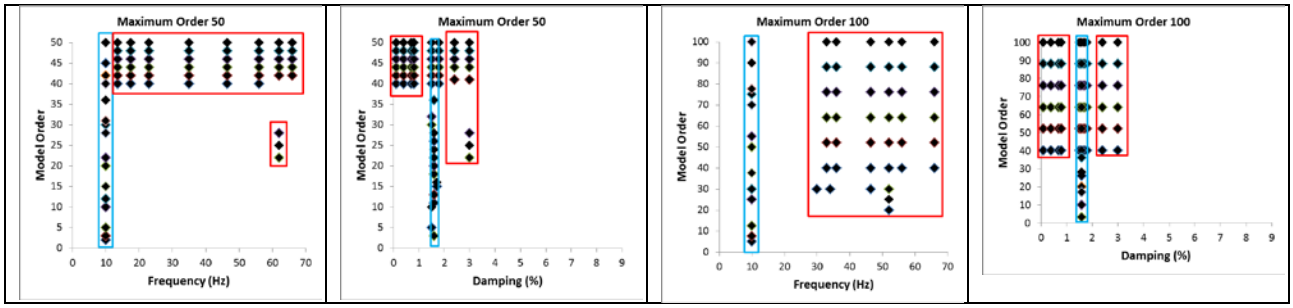

Figure 8: Accuracy vs. System Order

Fictitious modes are rather easy to detect but their important number and their appearance at lower model orders can make the analysis more complicated for the user. Like Vandermonde matrixes, the ad-hoc tuning requires several analyses to extract the maximum dynamics and minimize fictitious modes.

DOI: 10.13009/EUCASS2017-34

3.6 Synthesis

Results of these parametric studies are criterions based on the handiness of the OMA to be used as guide rules to maximize the efficiency and reliability of their applications (table 1).

Table 1: Handiness Criteria

Method	Handiness Criterion
Common to all methods	Time Slot Duration
	Minimum LSB
	Record Sampling Rates
Specific to HTM	Maximum of system order
Specific to SSI-f	Maximum of system order Vandermonde matrix factor
Specific to BR	Maximum of system order rank of Hankel matrix

As these criteria deeply depend of the phenomena encountered and registered in flight, they should be carefully checked before any use of the OMA algorithms: a blind application should be prohibited. We recommend as a safe rule to use systematically several OMA technics to strengthen the confidence on the results.

In the next paragraphs, we present the first attempt to deploy the four methods to flight measured signals.

3. First application on ARIANE 5 Flight Recorded Signal

First analysis were performed on a vibration transducer where main longitudinal modes on the Ariane 5 launchers can be observed. The transducer is recorded through all the flight phase. The solid rocket booster phase that corresponds also to the atmospheric phase is facing numerous external solicitations and perturbations which can be seen on the record (left part of figure 9). Some part of this flight phase are still eligible regarding OMA but we focused on the second part of the flight (Main Cryogenic Stage of Ariane 5 = EPC flight phase) where the sole Vulcain engine is source of a quasi-noise excitation (thrust noise). This part of about 350s is much more adapted for OMA.

Application of OMA put in evidence more than 10 clearly identified modes. Among them, we focused on the four first longitudinal modes (right part of figure 9). The end of the flight was not analysed as the frequency of the modes is shifting considerably which is penalizing the stationary conditions required by the analyses.

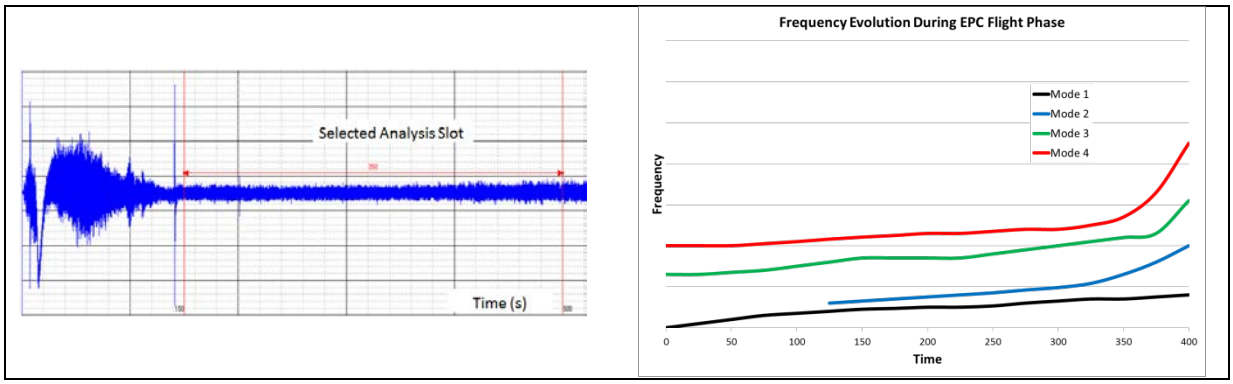

Figure 9: Analysed Signal and Frequency Content

Using handiness criterion, analysis were performed with four OMA algorithms, leading to damping assessment through time. The figure 10 presents different damping assessed form mode 2 and mode 3.

DOI: 10.13009/EUCASS2017-34

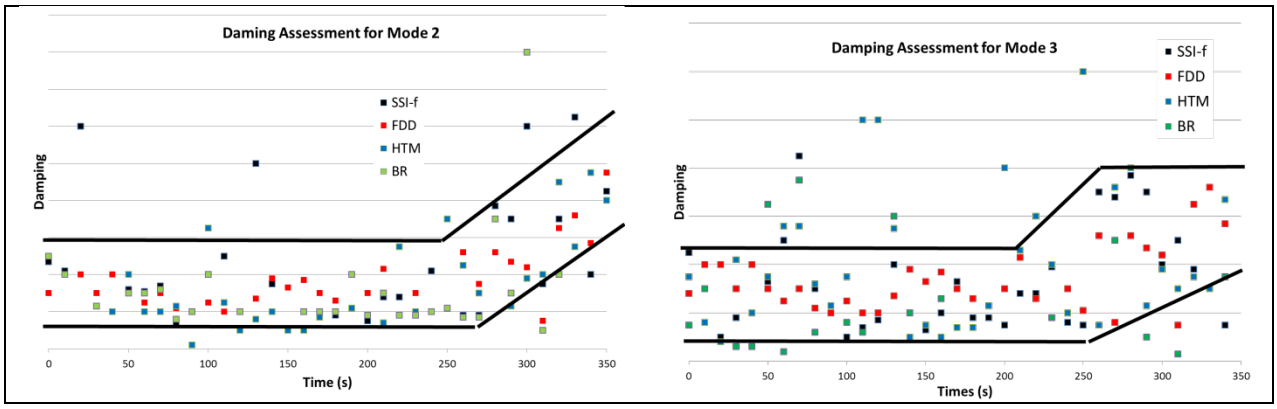

Figure 10: Damping Assessment Results

Regarding mode 2, damping estimation of the four algorithms provide the same order of magnitude and tendencies: an increase of damping at the end of the time slots. The scattering are globally significant with an envelope (bolted lines) of damping values at +/-50% of the average values. This must be balanced by the conditions of records that are definitively not comparable to ground conditions. Increase of records quality (through more adapted measurement ranges and larger bandwidth) is a key issue that will have to be tackled for future launcher developments.

Scattering observed on mode 3 are comparable to mode 2 but increase in the last part of analysed measurement. This is likely the combined effect of proximity of mode 3 and 4 and frequency evolution speed. A positive point is that results reached by the four methods are convergent which gives confidence to the measured values. Conversely, figure 11 showing the results reached for the mode 4 cannot be kept as reliable, the four algorithms giving too much chaotic evolutions with no clear tendency in the damping values. Such reliability assessment can only be performed using several methods: crosscheck of results is a major validation element of the credibility of outputs.

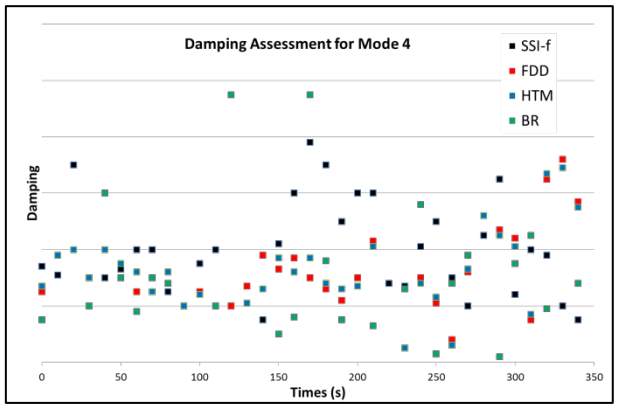

Figure 11: Unreliable Damping Assessment Results

Even with such crude experienced accuracy, estimations are still useful as they can be compared with minimum value used for mechanical vibrations forecasts, POGO and control stability analyses. They help quantifying existing margins and pointing out structures whose deformation is more damped than expected which are valuable lessons learnt.

In an operational perspective, demonstration of margins can be used to pronounce production clearances and eventually to extend the qualified domain using such margins.

Further analyses are still under progress to optimize treatment, select more adapted records and time slot analysis and extend the analysis to the large flight database available on Ariane 5.

DOI: 10.13009/EUCASS2017-34

4. Concluding Remarks

OMA approaches were benchmarked through a cooperation work between La Sapienza University and Airbus Safran Launchers. Four selected OMA algorithms have been used in order to identify the dynamic properties of a launch vehicle in terms of natural frequencies and damping ratios, considering the dynamical system under its actual operative conditions.

The robustness of BR, HTM, SSI and SSI-f algorithms was assessed w.r.t. in-operation measurement coarse quality. Handiness criterion were then established, that can be used by the user in order to reach reliable results when applied to typical launcher flight measurements.

First use of OMA was done on vibration measurement of the Ariane 5 launcher and gives encouraging results but uncertainties on damping remain significant. Further use of the analysis on the vast flight measurement database will be performed and will allow releasing relevant lessons learnt on in-flight damping. Complementary data treatment will be also led to enlarge the domain of use of these techniques.

References

[1] Goursat M., Basseville M., Benveniste A., Mevel L. 2001. Output-Only Modal Analysis of Ariane 5 Launcher. Proceedings of the 2001 IMAC-XIX: A Conference & Exposition on Structural Dynamics, Kissimmee, FL

[2] Gouache T., Morlier J., Michon G., Coulange B. 2013. Operational Modal Analysis with Non Stationary Input. IOMAC 2013, 12-15 may 2013, Guimaraes, Portugal

[3] De Vivo A., Brutti C., Leofanti J.L. 2014.Vega In-Flight Modal Identification with the Operational Modal Analysis Technique. Journal of Spacecraft and Rockets, Vol 51, No. 5, September-October 2014

[4] Eugeni M., Coppotelli G., Mastroddi F., Gaudenzi P., Muller S., Troclet B. 2017. OMA Analysis of a Launcher under Operational Conditions with Time-Varying Properties. 58th AIAA/ASCE/AHS/ASC Structures, Structural Dynamics, and Materials Conference, AIAA SciTech Forum, 2017

[5] Calvo L.M.E., Castellanos G.A., Portillo I.A. 2013. Application of Operational Modal Analysis on Railway Vehicles Using on Track Measurements. 2013 Joint Rail Conference, Knoxville, Tennessee, USA, April 15–18, 2013

[6] James G., Kaouk M., Cao T., Fogt V., Rocha R., Schultz K., Tucker J.M., Rayos E., Bell J., Alldredge D., Howsman T. 2012. Operational Analysis in the Launch Environment. Topics in Modal Analysis I, Volume 5. Conference Proceedings of the Society for Experimental Mechanics Series. Springer, New York, NY, 2012

[7] Coppotelli G., Grappasonni C., Di Trapani C. 2011. Dynamic Identification of a Solid Rocket Motor from Firing Test Using Operational Modal Analysis. 52nd AIAA/ASME/ASCE/AHS/ASC Structures, Structural Dynamics and Materials, 4-7 April 2011, Denver, Colorado, USA

[8] Durin G., Bouvier F., Mastrangelo G., Robert E. 2011. ARIANE 5 Solid Rocket Booster Dynamic Behavior with Respect to Pressure Oscillations. Progress in Propulsion Physics 2 (2011) 149-162

[9] Brincker R., Zhang L., Andersen P. 2000. Modal Identification from Ambient Responses using Frequency Domain Decomposition. Proceedings of XVIII International Modal Analysis Conference, IMAC, San Antonio, TX (USA), 2000.

[10] Agneni A., Balis Crema L., Coppotelli G. 2005. Output-Only Analysis of Coupled-Mode Structures. 1st International Operational Modal Analysis Conference, April 26-27, 2005, Copenhagen, Denmark

[11] Van Overschee P., De Moor B. 1996. Subspace Identification for Linear Systems. Kluver Academic Publisher, 1996.

[12] Louaas E., Chemoul B., Mourey P. 2004. Testing Philosophy for ARIANE 5 Structures Qualification Through Recent Examples. Proceedings of the 5th International Symposium on Environmental Testing for Space Programmes, Juine 15-17 2004, Noordwijk, The Netherlands